

# Radiocatalyst for Radiation Protection and Microbial Control

Michael Flynn<sup>1</sup>

*NASA Ames Research Center, Moffett Field, CA, 94035*

Rocco Mancinelli<sup>2</sup>

*Bay Area Environmental Research Institute, Moffett Field, CA, 94035*

Samuel Solomon<sup>3</sup>

*Massachusetts Institute of Technology, Cambridge, MA, 02139  
and*

Jordyn Garland<sup>4</sup>

*Kentucky Wesleyan College, Owensboro, KY, 42301*

Radiocatalysts are materials that reduce the activation energy required to split water into hydrogen and reactive oxygen species (ROS). They are activated by radiation and can be used to improve the ability of water to act as a radiation barrier. This paper reports the results of an experimental evaluation of a gold radiocatalyst. This work provides a preliminary evaluation of the ability of these types of catalysts to increase the efficiency of water hydrolysis when exposed to different types of radiation (GCR). Although the radiation exposure devices used in this testing were not capable of generating radiation as diverse as is commonly found in space, the testing is useful in evaluating the function of these radiocatalytic nanoparticles when exposed to a subset of the types of radiation that are found in GCR. The results are relevant to evaluating the use of this material for both space radiation protection and the production of useful byproducts, such as ROS, which can be used to maintain the sterility of stored water supplies. Radiocatalysts are materials typically used in radiation cancer therapy to improve the kill rate of tumors. These nanoparticles can be directly injected into tumors or functionalized to enter tumor cells via the blood stream. When they are exposed to radiation, they produce ROS. ROS are water hydrolysis products such as OH<sup>•</sup>, O<sup>•</sup>, O<sub>3</sub>, H<sub>2</sub>O<sub>2</sub>. This study used radiocatalytic 1.8 nm gold nanoparticles functionalized with citrate. These nanoparticles were tested through exposure to X-rays, <sup>56</sup>Fe particles and gamma rays to demonstrate activity to a variety of radiation sources. The results demonstrate that radiocatalysts can improve the radiation absorption of water by a factor of 3 to 8 and can effectively kill bacteria at radiation levels above 1 Gy.

## Nomenclature

ROS	=	reactive oxygen species
OH <sup>-</sup>	=	hydroxide ion
O <sup>•</sup>	=	molecular oxygen
O <sub>3</sub>	=	ozone
H <sub>2</sub> O <sub>2</sub>	=	hydrogen peroxide
Fe	=	iron
Gy	=	gray
BNL	=	Brookhaven National Laboratory
NSRL	=	NASA Space Radiation Laboratory
H <sub>2</sub> O	=	Water
DI	=	deionized water
AuNP	=	gold nanoparticles

---

<sup>1</sup> Physical Scientist, Bioengineering Branch, Ames Research Center, MS 239-11 Moffett Field, CA 94035

<sup>2</sup> Senior Research Scientist, Exobiology Branch, MS 239-14, Moffett Field, CA 94035

<sup>3</sup> Undergraduate Student, Massachusetts Institute of Technology, Cambridge, MA, 02139

<sup>4</sup> Undergraduate Student, Kentucky Wesleyan College, Owensboro, KY, 42301

GCR = galactic cosmic radiation

## I. Introduction

DEEP and cislunar space is characterized by the presence of galactic and solar radiation. This radiation represents a risk to human health and can damage spacecraft electronic components. It also provides an in situ resource that can produce reactive oxygen species (ROS) from water. However, the activation energy of water splitting reactions is high and although space radiation partials are relatively high energy their numbers are comparatively low resulting in a low intensity energy source. As the production of ROS is one of the main pathways through which water absorbs radiation, by reducing the activation energy of ROS production one can increase the absorption of radiation by water. Radiocatalysts are materials that can be used to reduce the activation energy of the water splitting reaction<sup>1</sup>. The production of ROS can additionally provide a in situ resource. ROS are commonly used as a biocide and when produced in a radiation protection water wall or storage tank they will act to keep the water sterile.

## II. Technical Approach

The mechanism of radiocatalytic function is a subject of debate but most theories are based on the disturbance of an electron valence by interactions with radiation and the resulting filling of an inner-shell vacancy of an atom which results in the emission of an electron. When an electron is excited and move to a higher valency, it leaves a vacancy at the lower valence and an electron from a higher energy level can fall back into the vacancy resulting in a release of energy from the surface of the nanoparticles. This release of energy leads to the reaction resulting in the creation of ROS.<sup>2</sup> Electron-hole pair yields of 10 to 100 per keV of absorbed radiation for typical semiconductors is possible.<sup>3</sup> Medical radiation therapy has been using radiocatalysts for many years with X-rays and gamma rays.<sup>4</sup> Recently, therapies using proton and particle beams have been developed that use gold and titanium radiocatalysts.<sup>2,5, 6, 7 & 8</sup>

This paper describes the results of an experimental study using 1.8 nm gold nanoparticles to improve the ability of water to absorb radiation and produce ROS. The produced ROS are then evaluated for their ability to kill bacteria and maintain the sterility of the water. The nanoparticles were exposed to X-rays, gamma rays and high energy particles in order to evaluate changes in oxidation-sensitive fluorophores and kill rates of bacteria. The relative florescence intensity and optical density after exposure correlates to the radiation absorption and bacterial growth respectively. Data was generated relevant to both the ability of the catalyst to improve the radiation protection characteristics of water and as an in situ resource for the production of ROS. This testing did not simulate the full spectrum of radiation sources in GCR but only a subset for this preliminary feasibility evaluation. The ability of the nanoparticles to generate ROS in order to kill microbes was tested using X-rays and reactive nuclei. A low intensity gamma ray source was used to evaluate the function of the radiocatalyst at low radiation levels.

## III. Materials and Methods

This study used functionalized gold nanoparticles purchased from NanPartz Inc. These 1.8nm citrate capped gold nanoparticles are shown in Figure 1. Functionalization of the nanoparticles with citrate is done by directly attaching the citrate molecule to the surface of the particle. Citrate is used to stabilize the nano-particles and allow the 1.8nm particles to pass through a bacteria's cellular membrane. The citrate cap also helps to prevent the particles from agglomerating into larger particles. The 1.8nm particles used in this study are not stable by themselves and have to be functionalized or they will spontaneously combine to form larger particles. Two samples of 1.8nm citrate capped AuNP were used. One was used for the testing and the other was stored at room temperature for 11 months and used to evaluate the catalyst's stability.

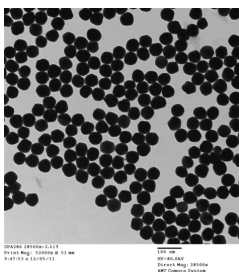


**Figure 1. 1.8 nm gold nanoparticles**

The gold particles shown in Figure 1 were mixed with water and exposed to three different types of radiation: X-rays, gamma rays, and <sup>56</sup>Fe. The X-rays were generated from an X-Rad iR160 source at 1.2 Gy/min. The gamma rays were generated by a 0.4 mGy/hr cesium epoxy laminate gamma ray source. The <sup>56</sup>Fe was provided at 600 MeV/n at the Brookhaven National Laboratory (BNL) NASA Space Radiation Laboratory (NSRL). The X-rays and gamma ray exposures were conducted in 96 well plates while the <sup>56</sup>Fe exposures were conducted in 4 ml cuvettes. The selection of radiation sources

and minimum intensities was dictated by the availability of equipment at NASA Ames Research Center and the NSRL at the time of testing.

The production of ROS was measured through the use of a fluorescent probe, which is an organic fluorescent dye that is easily oxidized by ROS. As the dye oxidizes, the fluorescence decreases. Two fluorescent probes were chosen from literature, fluorescein and Coumarin-3-carboxylic Acid. After evaluating the different fluorescence probes, Fluorescein was chosen for further testing due to its lower sensitivity. Fluorescein has an excitation at 494 nm and emission at 512 nm. The fluorescein calibration curve for hydrogen peroxide is provided in Figure 2. This Figure shows that the fluorescein has a sensitivity limit at about  $20^{-3}$  molar  $H_2O_2$  and decays exponentially.

Microbial growth experiments were conducted using optical density as a measurement of bacterial populations. Microbial samples were exposed to radiation and then incubated and optical density measured as a function of time to produce growth curves.

### A. Experimental Protocol

The following protocol is specific for the  $^{56}Fe$  exposures completed at BNL but are essentially the same for X rays and gamma ray exposure, except that a 97 well plates were used in place of the 4 ml cuvettes.

#### *Preparation of the $H_2O$ Blank:*

50 mL of DI H<sub>2</sub>O was placed into a 125 mL Erlenmeyer flask. 2 uL of 25 uM Fluorescein (9.4 mg of Fluorescein (376.27 g/mol) into 1 L of DI water) was added to the flask to create a final concentration of 1 nM Fluorescein solution in 50 mL DI H<sub>2</sub>O. 3 mL of the Fluorescein blank were placed into 5 separate cuvettes and exposed to 0, 0.1, 1, & 10 Gy.

#### *Preparation of the $H_2O$ Nanoparticle Solution:*

50 mL of DI H<sub>2</sub>O was placed into three separate 125 mL Erlenmeyer flasks. 2 uL of 25 uM Fluorescein (9.4 mg of Fluorescein (376.27 g/mol) into 1 L of DI water) was added to each of the flasks to create a final concentration of 1 nM Fluorescein solution in 50 mL DI H<sub>2</sub>O. 1 uL of AuNP (0.1 ug/mL AuNP) was placed in a flask. 10 uL of AuNP (0.1 ug/mL AuNP) was placed in another flask. 100 uL of AuNP (0.1 ug/mL AuNP) was placed in another flask. Each of the three flasks were then subdivided into five plastic polyethylene cuvettes.

#### *Preparation of LB Media:*

10g of LB broth was placed into 400 mL of DI H<sub>2</sub>O and autoclaved. After the media cooled down, 400 uL of carbenicillin was added to the media for a final concentration of 100 ug/mL of carbenicillin.

#### *Cell Culture and Exposure:*

Swipe three isolated colonies from the agar plate and drop the stick inside the media flasks. Incubate the media overnight at 37 °C rotating at 180 RPM. Next day: Autoclave 50 mL of fresh media into six 125 mL flasks (25 g LB Broth, 1 L DI H<sub>2</sub>O). Place 50 uL of carbenicillin into each flask. Place six 50 mL media flasks, sterile holders (for 8-tip pipet), cuvettes, overnight cell culture media (a), and 100/10 uL cuvette tips inside the hood. Place 3 mL of media solution into a plastic polyethylene cuvettes. Add 200 uL of overnight cell media into fresh media flasks. Place 3 mL of solution into each of five rigid plastic polyethylene cuvette. Place lid on top of cuvette and seal with tap. Add 100 uL of AuNP (OD 100, 5 mg/mL) into fresh media flask (10 ug/mL AuNP). Place 3 mL of solution into each of four rigid plastic polyethylene cuvette. Add 200 uL of overnight cell media into fresh media flask F. Add 1 uL of AuNP into flask F (0.1 ug/mL AuNP). Add 200 uL of overnight cell media into fresh media flask. Add 10 uL of AuNP into flask (1 ug/mL AuNP). Place 3 mL of solution into each of four rigid plastic polyethylene cuvettes. Add 200 uL of

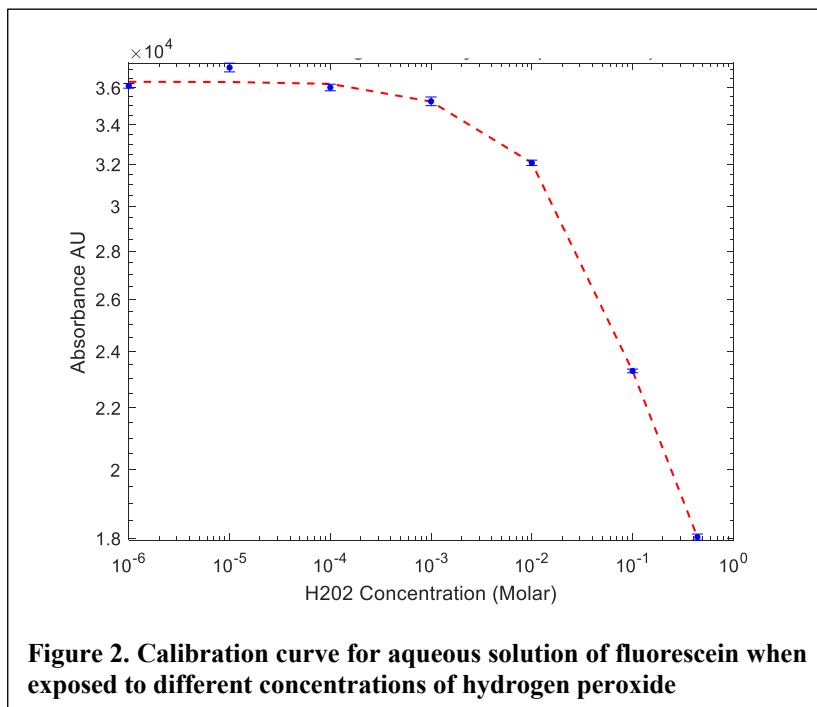


**Figure 2. Calibration curve for aqueous solution of fluorescein when exposed to different concentrations of hydrogen peroxide**

overnight cell media into fresh media flask. Add 100 uL of AuNP into flask H (10 ug/mL AuNP. Place 3 ml of solution into each of four rigid plastic polyethylene cuvettes.

Measure fluorescence of all cuvettes before exposure. Measure OD of all cuvettes before exposure. Provide cuvettes to BNL staff for exposure 0Gr, 0.1Gr (at 0.26 Gy/min), 1Gr (at 1.0 Gy/min) and 10Gr (at 1.2 Gy/min) using 600 MeV/u  $^{56}\text{Fe}$  source.

Measure fluorescence of all relevant and measure OD of all relevant cuvettes immediately after exposure. Then every hour thereafter repeat measurements of fluorescents for 4 hours. Then every 2 hours thereafter, repeat measurements of OD for 24 hour

For E. coli growth studies, plates were refrigerated prior to exposure and incubated at 37°C after exposure. During the BNL exposures there was indication that some of the cuvettes may have leaked during shipment. When samples were returned after the  $^{56}\text{Fe}$  exposures they were radioactive. This means that the control was exposed to low levels radiation in the incubator.

X ray exposures were completed in 97 well plates in a X-Rad IR160 at 1.2 Gy/min. Exposures lasted from seconds to minutes. Gamma ray exposures were completed in 97 well plates using a 0.4 mGy/hr cesium epoxy tile. Exposures lasted from days to a week to accumulate a dose high enough to be detected by the fluorescence detector. The well plate was sealed with a lid and the effect of evaporation was monitored by a fluorescent blank row in each well plate.

## B. Results

The key hypothesis of this research is that radiocatalysts improve the ability of water to absorb radiation by producing ROS. This was tested by exposing aqueous solutions of gold nanoparticles to radiation. The solutions included a fluorescent probe that was sensitive to ROS generation. The reduction in relative fluorescence due to ROS generation in samples exposed to radiation was used to correlate to the radiation absorption capacity of water. Figure 3 shows the change in relative fluorescence of aqueous samples exposed to X rays, with and without a radiocatalyst.

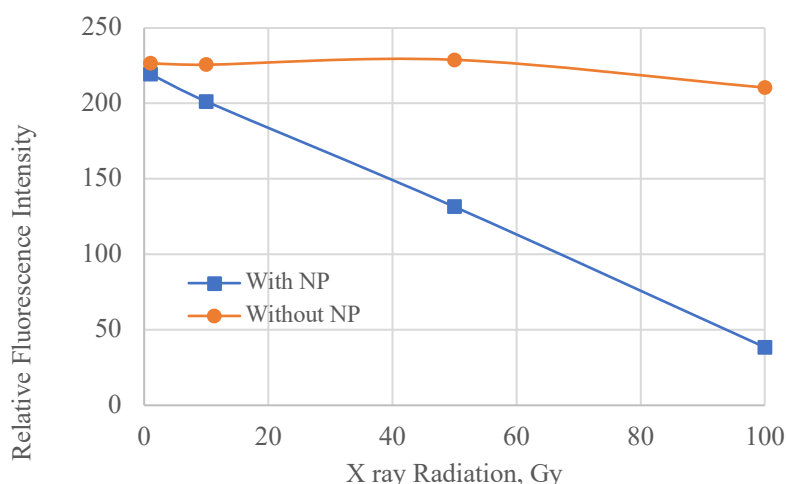


**Figure 3. Change in relative fluorescence intensity as a function of X ray exposure.**

As shown in Figure 3, the addition of the radiocatalyst changes the relative fluorescent intensity of the sample when exposed to X rays. These results indicate that the radiocatalyst can improve the absorption capability of water by as much as 5 times, at the maximum exposure of 100 Gy. At lower adsorptions, near the zero, the fluorescent probe sensitivity flattens out as shown in the calibration curve, see Figure 2. The exposures shown in Figure 3 are well above any radiation levels that will be encountered in space. Although X-rays and gamma rays can be intense for short periods of time, such as during solar particle events, the consistent background energy levels are low. Inside a spacecraft outside of Low Earth Orbit, radiation levels of around 0.4 Gy per year (or 0.05 mGy/hr) can be expected and X-rays only compose a small fraction of this radiation.<sup>9 & 10</sup> The bulk of the energy content from space background radiation comes from galactic radiation (protons and ionized nuclei). Figure 4 shows the change in relative fluorescence intensity for exposures to  $^{56}\text{Fe}$  particles.  $^{56}\text{Fe}$  particles are the most common isotope of iron. Figure 4 shows that at 0.1 Gy the radiation absorption capability of water is improved by a factor of about 8.

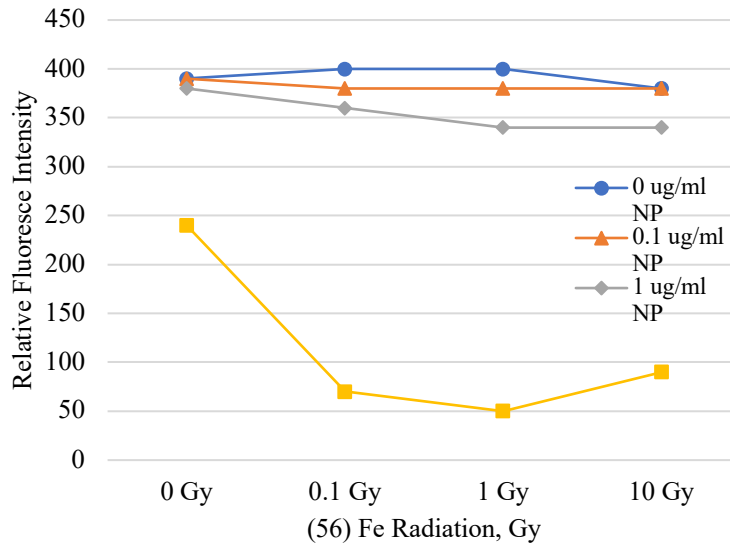


**Figure 4. Change in relative fluorescence intensity as a function of  $^{56}\text{Fe}$  exposure**

Testing with high intensity short duration exposures, such as shown in Figures 3 and 4, are not a very realistic simulation of space radiation. Space radiation is composed of high energy particles at low densities, so dose rates are a function of time. The X ray and  $^{56}\text{Fe}$  sources, used in Figure 3 and 4, were high intensity sources so exposure times were short. To more accurately simulate GCR a very low energy source is required that is used to complete longer duration exposures, up to 0.4 Gy/Yr. This requirement for long duration exposures requires exposures to a dedicated low intensity radiation source for a long period of time. Testing with a low intensity cesium epoxy laminate 0.4 mGy/hr gamma ray source was completed to provide a simulation of low intensity long duration exposure. Figure 5 shows the change in relative florescence for this low intensity gamma ray source. At 0.13Gy there was about a factor of 3 improvement in the adsorption of gamma rays by water. Although gamma radiation is only small contributor to GCR, the results in Figure 5 show that the radiocatalyst is active at radiation levels in the range that is encountered in space. Note that the difference in magnitude in the fluorescent signal in Figure 5 compared to that in Figures 3 and 4 is the results of the use of a more sensitive fluorometer

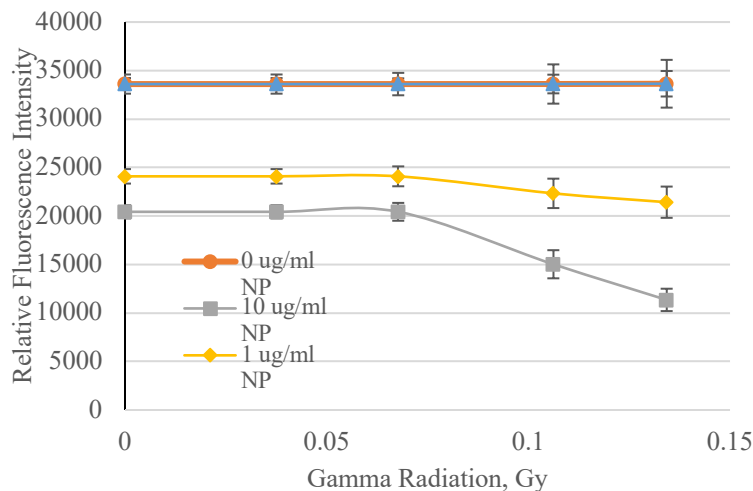
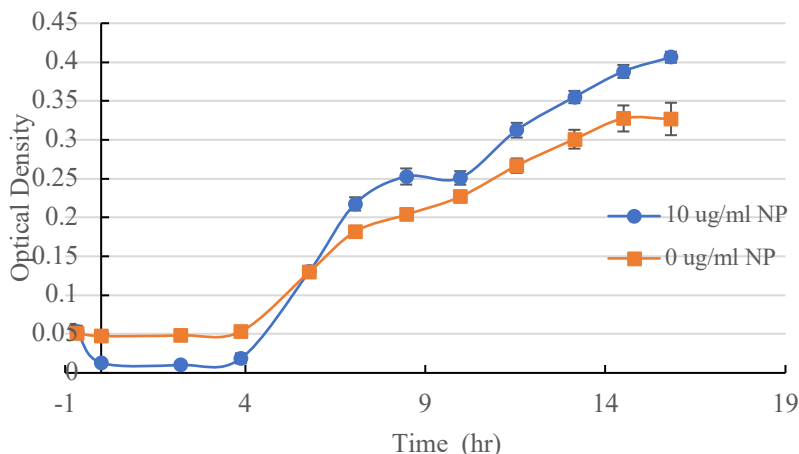


**Figure 5. Change in relative fluorescence intensity as a function of gamma ray exposure.**

### C. In situ resource utilization

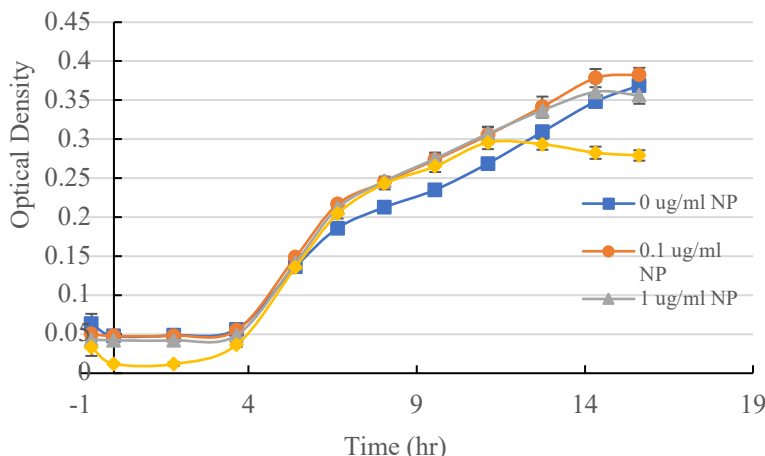
One of the unique aspects of radiocatalysts is that they provide a method of using space radiation as an in situ resource. Space radiation offers an energy source to produce ROS. ROS can be used to complete other useful work. In this study the use of the produced ROS was evaluated as a biocide to kill bacteria and ensure the sterility of the stored spacecraft water within which it is contained.

Figure 6 provides a growth curve for E coli when exposed to radiation with and without the radiocatalysts. The exposure to radiation occurred before time zero. At time 0 the exposure to X rays with nanoparticles initially kills greater than 90% of the bacteria, when compared to exposure without nanoparticles, but then with time the bacteria grow back and resume a normal growth curve. The samples are not completely sterilized but the starting population is significantly reduced and the lag phase is extended. Later in the log and stationary phase of the curve the trend is reversed and the samples with nanoparticles have improved growth rates and higher final concentrations.



**Figure 6. E. coli Growth Curve After Exposure to 10 Gy X Ray With 0 ug/ml and 10 ug/ml AuNP**

Ten Gy is a considerable higher radiation level than would be expected in space. Figure 7 presents a growth curve at 1 Gy with 3 different nanoparticle concentrations. The Figure shows a similar kill rate at the initial exposure and extended lag phase. The Figure also shows that the kill rate is a function of the nanoparticle concentrations. This supports the hypothesis that the kill rate is a function of the ability of the nanoparticles to enter into the cells and produce ROS internally rather than generally raising the oxidation potential of the growth media. The situation reverses in the log and stationary phases and the nanoparticles again have improved growth rates.



**Figure 7. E. coli Growth Curve After Exposure to 1 Gy X Rays with 0, 0.1, 1, and 10 ug/ml AuNP**

Experiments at exposures below 1 Gy were not possible with the X-Rad IR160 X ray source. To get exposures below 1 Gy the  $^{56}\text{Fe}$  source at BNL was utilized. Figure 8 presents the results from this low intensity  $^{56}\text{Fe}$  exposure. As show in the Figure the initial kill rate is lower than in the 1 Gy and 10 Gy X ray exposures and the lag phase is not delayed.

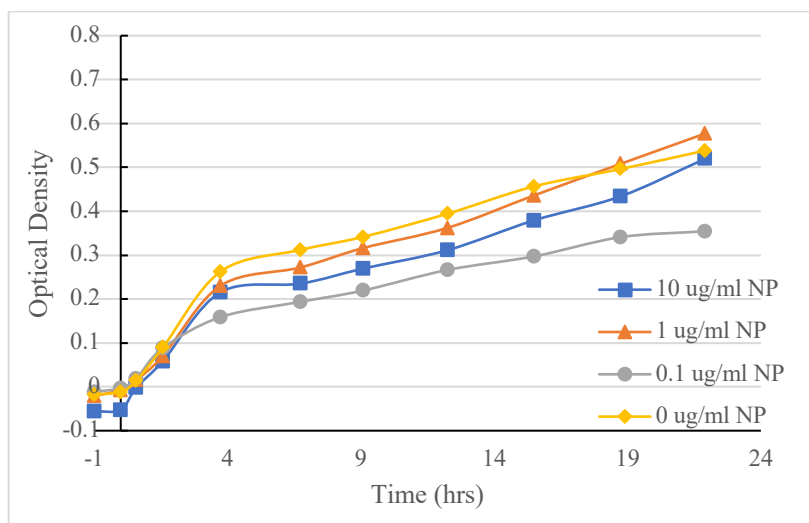


**Figure 8. E. coli Growth Curve After Exposure to 0.1 Gy ( $^{56}\text{Fe}$ ) with 0, 0.1, 1, and 10 ug/ml AuNP**

Exposures below 0.1Gy were not possible at BNL or using the X ray source. The gamma ray source was capable of conducting low dose exposures but the exposure device could not be used with bacteria due to possible contamination by the E coli. The gamma ray source was used primarily for mammalian cell culture exposures so sterility is critical.

#### D. Nanoparticle stability

As stated earlier two samples of gold nanoparticles were purchased. One was used for the testing and the other was stored at room temperature for 10 months. Near the end of the program these two samples were tested in the gamma ray exposure device, side by side, to evaluate their stability. Figure 9 presents the results of this stability test. The Figure shows that the nanoparticles stored for 10 months at room temperature had lower reduction in relative florescence that the nano particles that were less than 3 months old and stored under refrigeration.

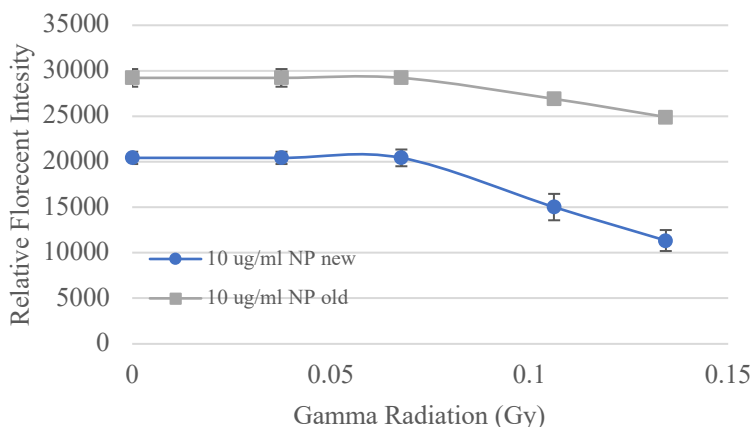


**Figure 9. Change in Relative Fluoresce Intensity as a Function of Gamma Ray Exposure for New Verses Old Nanoparticles.**

#### IV. Conclusion

As shown in Figure 3, 4, 5 and 9, radiocatalysts improve the ability of water to absorb radiation. The degree to which this improvement occurs is primarily a function of the concentration of nanoparticles. For X rays a maximum of 5 times improvement in absorption over water with no nanoparticles was measured. X ray absorption increased with radiation dose. For  $^{56}\text{Fe}$  exposures an 8 times improvement over water was measured and the adsorption did not increase substantially with dose. For low intensity gamma rays, a 3 times improvement over water alone was measured and the absorption increased with dose. The equipment used in this study was not capable of providing an accurate simulation of the full complexity or intensity of GCR radiation. As a result, the approach used was to demonstrate activity of the radiocatalyst to three different types of radiation found in GCR, X rays, gamma rays and  $^{56}\text{Fe}$  particles and for  $^{56}\text{Fe}$  and gamma rays to test in the range of expected GCR intensities. Although more work is required, the results indicate that the radiocatalyst is active across the three types of radiation sources tested and at intensity levels similar to GCR for  $^{56}\text{Fe}$  and gamma rays. Although more work will be required to fully evaluate the radiocatalyst performance to real GCR, these preliminary results are promising.

Figures 5 and 6 show that gold radiocatalysts can be used to kill bacteria in water. However, at the catalyst concentrations and radiation levels used in this study the kill rate is not high enough to sterilize the samples. Although there was a significant kill at the time of exposure, the samples were not sterilized and the bacteria did grow back. In many cases the grow back appeared to actually be enhanced by the presence of the nano particles. Figure 7 demonstrates that at 0.1 Gy the effect of the radiation exposure with nanoparticles is minimal. The kill rate is very low and the extension of the lag phase in almost nonexistent.

It has also been demonstrated in Figure 8 that the 1.8 nm gold nanoparticles are not stable over time. The citrate functionalization decomposes and the particles agglomerate into larger particles and thus the concentration decreases with time. Figure 8 shows that the performance of 1.8 nm particles decreased over the 11 months.

#### V. Discussion

Based on this preliminary research, the use of radiocatalyst in water-based shielding architectures could significantly reduce the amount of water required to provide radiation protection. Although this work did not attempt to accurately simulate GCR in all its complexity, it did demonstrate the functionality of a radiocatalyst when exposed three different types of radiation. The relatively high X ray and  $^{56}\text{Fe}$  radiation minimum intensity levels were set by the radiation sources themselves. The gamma ray source, which is not a big component of GCR, was the only source capable of providing intensities within the time dependent range of GCR. Taken together the results of this work provide a preliminary indication that the radiocatalyst is applicable to different types of radiation and is functional at low radiation intensities.

It is likely that with more research additional improvements in radiation absorption could be realized. The data from this study has shown that that increasing the concentration of the catalyst improves the overall absorption performance. Our study did not identify the optimal concentration but showed improvement for all types of radiation based on catalyst concentration. In addition, we did not try and optimize the catalyst as part of this work. We used a commercially available gold catalyst. A review of the relevant literature indicates that a platinum radiocatalysts provides an improvement over gold.<sup>8 & 12</sup> It has been shown that surface roughness, size and shape of the nanoparticle also plays an important role in catalyst function.<sup>12 & 14</sup>

The stability of the nanoparticles will also need to be optimized. At the 1.8 nm size the particles are unstable and surface functionalization is required to keep them from agglomerating into larger particles. Based on data provided by the manufacture, catalyst sizes between 150 and 300 nm are stable. While this does not present a problem for use of the catalyst for radiation protection, it may present a problem for use of the catalyst for maintaining the sterility of spacecraft water systems. For the radiocatalyst to be effective at killing bacteria the nanoparticles must be smaller than the bacteria, so that it can pass through the bacteria's cell membrane and enter the cell.

Although the catalyst can be optimized to improve its ability to adsorb radiation, this study has shown that the use of the resulting ROS as an in situ resource is not possible. The energy contained in background space radiation is just too low. There are also issues with bacteria adapting to survive low levels of ROS and this work has shown that there is even the potential for accelerated growth at the low levels of ROS studied.



## VI. Acknowledgments

The authors would like to acknowledge the support provides by the NASA Advanced Exploration Systems, Advanced Life Support, High Risk High Reward funding.

## VII. References

- <sup>1</sup> Gilles M., E. Brun, C. Sicard-Roselli <sup>†</sup>, Quantification of hydroxyl radicals and solvated electrons produced by irradiated gold nanoparticles suggests a crucial role of interfacial water, *Journal of Colloid and Interface Science* 525 (2018) 31–38
- <sup>2</sup> Jeynes, J C G, M. J. Merchant, A. Spindler, A-C. Wera and K. J. Kirkby, Investigation of gold nanoparticle radiosensitization mechanisms using a free radical scavenger and protons of different energies, *Phys. Med. Biol.* 59 (2014) 6431–6443
- <sup>3</sup> Verkhovtsev, A. V., A. V. Korol, and A. V. Solov'yov, Revealing the Mechanism of the Low-Energy Electron Yield Enhancement from Sensitizing Nanoparticles, *PRL* 114, 063401 (2015)
- <sup>4</sup> Kuncic, Z., and S. Lacombe, Nanoparticle radio-enhancement: principles, progress and application to cancer treatment, *Phys. Med. Biol.* 63 (2018) 02TR01 (27pp)
- <sup>5</sup> Liu, Y., Xi Liu, X. Jin, P. He, X. Zheng, et al, The dependence of radiation enhancement effect on the concentration of gold nanoparticles exposed to low- and high-LET radiations, *Physica Medica* 31 (2015) 210e218
- <sup>6</sup> Lacombe, S., E. Porcell and E. Scifoni, Particle therapy and nanomedicine: state of art and research perspectives, *Lacombe et al. Cancer Nano* (2017) 8:9
- <sup>7</sup> Li1, S., S. Penninckx, L. Karmani, A. Heuskin, et al, LET-dependent radiosensitization effects of gold nanoparticles for proton irradiation, *Nanotechnology* 27 (2016) 455101 (9pp)
- <sup>8</sup> Porcel, E., S Liehn, H. Remita, N. Usami, K. Kobayashi, Y. Furusawa, C., L. Sech and S. Lacombe, Platinum nanoparticles: a promising material for future cancer therapy, *Nanotechnology* 21 (2010) 085103 (7pp)
- <sup>9</sup> Mewaldta, R.A., A.J. Davisa, W.R. Binnsb, G.A. de Nolfoc, J.S. Georged, M.H. Israelb, et al, The Cosmic Ray Radiation Dose in Interplanetary Space – Present Day and Worst-Case Evaluations, 29th International Cosmic Ray Conference Pune (2005) 00, 101-104
- <sup>10</sup> Wu, X., T. Hamilton, D. J. Helfand, and Q. Wang, The intensity and spectrum of the diffuse X-Ray Background, *The Astrophysical Journal*, 379:564-575, 1991 October 1
- <sup>11</sup> Simonsen, L., J. E., Nealy, Radiation Protection for Humans Missions to the Moon and Mars, NASA Technical Paper 3079, February 1991, National Aeronautics and Space Administration.
- <sup>12</sup> Kuncic, Z., and S. Lacombe, Nanoparticle radio-enhancement: principles, progress and application to cancer treatment, *Phys. Med. Biol.* 63 (2018) 02TR01 (27pp)
- <sup>13</sup> Rosa S, C. Connolly, G. Schettino, K. T. Butterworth1 and K. M. Prise1, Biological mechanisms of gold nanoparticle radiosensitization, *Cancer Nano* (2017) 8:2
- <sup>14</sup> Walzlein, C., E Scifoni, M Krämer and M Durante, Simulations of dose enhancement for heavy atom nanoparticles irradiated by protons, 2014 *Phys. Med. Biol.* 59 1441